International Journal of Scientific Research and Engineering Development-– Volume 6 Issue 5, Sept-Oct 2023

Available at www.ijsred.com

RESEARCH ARTICLE OPEN ACCESS

LCL Filter with Giant Trevally Optimizer Based Three-Phase Grid Connected Inverter

R.Ann Roshny*, Dr.M.Suthanthira**

*(Department of Electrical and Electronics Engineering, Arunachala College of Engineering for Women, and Manavilai, Vellichanthai

Email: annroshnyr20@gmail.com)

** (Department of Electrical and Electronics Engineering, Arunachala College of Engineering for Women, and Manavilai, Vellichanthai

Email: suthanthiraabi@gmail.com)

----------**********----------

Abstract:

The three-phase grid-connected inverter system with controller design and implementation is presented in this study. It is based on the synchronous based theory, has a bus capacitor across the dc voltage at the input, and connects the LCL filter at the inverter's output. Due to the LCL filter's stronger filtering capabilities, we use it. The three-phase LCL-GCI (LCL-GCI) is a grid-connected inverter claims a higher demand to the control system design because it is a third-order and multi-variable system. A complicated space grid current vector under synchronous frame PI control in the dq reference frame is the control strategy employed. The majority of these algorithms take their cues from the animal kingdom's collective intelligence and hunting techniques. The LCL Filter with Giant Trevally Optimizer Based Three Phase Grid Connected Inverter is suggested in this study. The three key steps of the distinctive hunting tactics used by giant trevally to catch seabirds are mathematically modelled in this article. The first phase is imitating the massive trevallies' foraging movement patterns. The huge trevallies select a region that will provide them with food in order to seek for prey in the second step. The trevally starts chasing the seabird in the final phase. The trevally will jump out of the water and attack its food in the air or even snag it off the water's surface when it is sufficiently close to it. The impact of the controller's tuning settings is investigated using complex vector root locus and complex vector frequency response functions of closed loop systems in accordance with various tuning parameters. Additionally, the LCL filter is employed to eliminate THD in three-phase inverter with dq control connected to the grid. An effective optimizer for global optimisation is the proposed GTO. Utilising MATLAB Simulink, a control system and simulated three-phase grid-connected inverter.

Keywords **—Three phase grid-connected inverter,Grid-connected inverter, grid current control, and synchronous frame PI controller, GTO.**

----------**********----------

I. INTRODUCTION

This paper discusses the three-phase inverter's controller design and implementation. A three-phase inverter must be employed in order three-phase inverter with dq control connected to the grid. Since switching elements make up the inverter, the output that is produced depends on how the switching is carried out. This chapter explains the idea of a switching function and the corresponding switching matrix. Grid linked inverters (GCIs) play a larger role as an interface between the grid and distributed energy resources (DERs), as renewable energy sources continue to be integrated across the upgraded electrical infrastructure. The controller of

the GCI should be appropriately developed in order to get the desired performance from DERs. Reference stationary and synchronous frame PI regulators are compared in the frequency domain for voltage source inverters with current regulation. When a three-phase voltage-source inverter includes an outer control loop that regulates grid current and an interior control loop that regulates filter capacitor current, synchronous frame PI regulation is utilised. In order to further enhance the performance of regulators of current for ac loads and motors employing complicated vector, virtual translation technology is also used for ac machines.

To attain excellent power quality, a three-phase inverter is constructed with digital control, and a z-domain tuning method utilising the pole position strategy is suggested. The control methods and control strategies are offered when faults occur, depending on the reference frame. GCI is often implemented using a frame-synchronized PI controller and is modelled as a dq model using scalar notation. When scalar notation is employed, it is challenging to analyse a GCI system and adjust the gains of PI controllers. Complex vector notation makes it simpler to construct the controller and analyse the system while also reducing the system's order. A common method for regulating AC machines is the complex vector model. However, there haven't been many instances of it being used for GCI modelling. There are still opportunities to investigate the effects of tuning parameters to avoid instability and achieve outstanding grid current quality when GCI is described using complex vector notation. This study presents the sophisticated vector modelling of the grid current in the synchronous dq reference frame with the synchronous frame PI controller. Additionally, the adjusting of the controller's effects settings is examined utilising the three-phase GCI's complex vector root locus and complex vector frequency response function. When modelling GCI, the benefit of utilising complex vector notation is explained. Complex vector format is obtained from the closed-loop transfer function of the three-phase GCI with the synchronous frame PI controller.

II. PROPOSED METHODOLOGY

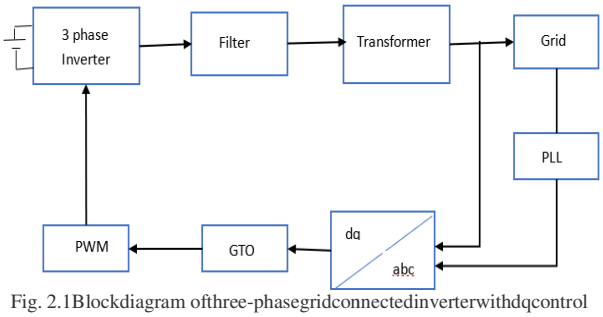

Fig. 2.1Blockdiagram ofthree-phasegridconnectedinverterwithdqcontrol

Fig 2.1 presents the block diagram of the grid-connected inverter system. The most popular arrangement for three phase systems is the complete bridge three phase inverter topology. The chosen inverter is a voltage source inverter with current control and an amplitude modulation index (ma) of 0.9. The switching component, which operates at a frequency of 20 KHz, is a MOSFET. The PWM is then linked here to the GTO. When using the bi-polar PWM approach, switches in each pair are simultaneously turned ON and OFF, and the output voltage fluctuates between -Vdc and +Vdc. Vdc is the input voltage of the inverter, which is thought of as the battery as indicated in the block diagram. Each leg's output is not influenced by load current but only by input voltage and switch condition.

A three-phase inverter connected to the grid system that includes both the design and use of a controller. It is based on the synchronous based theory, has a bus capacitor across the dc voltage at the input, and connects the LCL filter at the inverter's output. Figure 1 above depicts the block diagram of a three-phase inverter with dq control connected to the grid. It is founded on the principle of synchronous reference frames. A bus capacitor is placed across the input's dc voltage before it is linked to an inverter bridge comprised of an IGBT or a MOSFET. The LCL filter is then linked to the inverter's output. Because of its excellent filtering performance, we utilise LCL filter. Finally, the output is connected to a three-

phase, three-wire grid. We must first measure the voltages. These are the voltages from line to line. Then, using Park's transformation, these three phase abc voltages are converted to two phase alpha beta volts. This alpha-beta voltage is used to build the Phase Locked Loop (PLL). Then, using Clark's transformation, alpha beta voltages are changed into dq voltages. using the inverter side current in this case. Then, using Park's transformation, this current are converted to the alpha-beta domain. then moved into the dq domain. Here, active current is represented by id and reactive current by iq. Here GTO is connected to the PWM inverter. The PI controller then uses the error to determine the voltages Ud and Uq. The relationship between the modulation index and inverter voltage for a sine PWM modulation method. Finally, PWM generation is on the block.

A. *Giant Trevally Optimizer*

The suggested MA, known as the Giant Trevally Optimizer (GTO), which draws its inspiration from nature, is described in this section.

B. *Inspiration and Hunting Behaviour of the Giant Trevally*

A huge marine predator belonging to the jack family is the enormous trevally. It is also known as the enormous kingfish. The Indian and Pacific oceans are teeming with them. Typically silver in colour with a few dark patches, giant trevally. It can be identified by its pointed head, powerful tail scutes, and a variety of other physical features. They can weigh 80 kg and have a height of 170 cm. Fish, cephalopods, crabs, and seabirds make up their daily food. As the search area grows, literature has looked into how gigantic trevallies move within and across habitats. According to some research, adult giant trevallies migrate up to 9 kilometres each day and seasonally throughout their roving territory.

The gigantic trevally is a top predator and employs cunning hunting techniques in most of its habitats. It is known that the gigantic trevally hunts both solitary and in packs. The leader or first predator in a group or school is the most successful at acquiring prey. Over 500,000 terns congregate on one of the Indian Ocean's remote atolls during the dry season. It has been claimed that fifty enormous trevallies, drawn by the abundance of possible prey where the young terns begin to learn to fly, come from nearby reefs. The giant trevally marks its hunting territory before beginning to pursue (chase) its victim. It then leaps out of the water and attacks the prey (seabird). The fundamental design inspiration for the GTO came from these innovative hunting techniques, including as foraging movement patterns, selecting a region with sufficient taking flight from the water to attack and seize the victim.

C. *Modelling of a Three-Phase Grid Co[nnected Inverter Using Complex Vectors*

Diagram of a grid-connected three-phase PWM voltage source inverter seen via an LCL filter is shown in Fig 2.2. The following presumptions are taken into account:

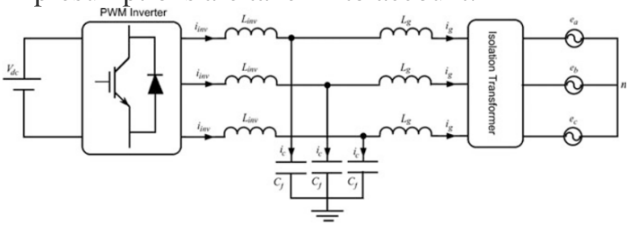

Fig. 2.2 Three-phase grid-connected PWM inverter with LCL-filter

1. None of the equivalent series resistance for the transformer inductor, grid-side filter inductor, inverter-side filter inductor, or filter capacitor is taken into account.
2. The essential components in the ac supply voltages are all in the positive sequence.

Applying these presumptions results in a per-phase equivalent circuit with s-domain transfer functions that represents the plant model Gp(s) at non-fundamental frequencies and simplifies Fig. 2 to that level. A model of the circuit is as follows:

$$L_{gt} = L_g + L_{tr} (1)$$

$$V_{inv}(s) = \left(L_{inv}s + \frac{1}{C_f s}\right) I_{inv}(S) - \left(\frac{1}{C_{fs}}\right) I_g(s) (2)$$

$$I_{inv}(s) = \left(L_g C_f s^2 + 1\right) I_g(s) (3)$$

By substituting Eq. (2) in (1), the Gp(s) can be expressed as:

$$G_p(s) = \frac{I_g(s)}{V_{inv}(s)} = \frac{1}{L_{inv}L_{gtc}^3{}_{fs} + (L_{inv} + L_{gt})s} (4)$$

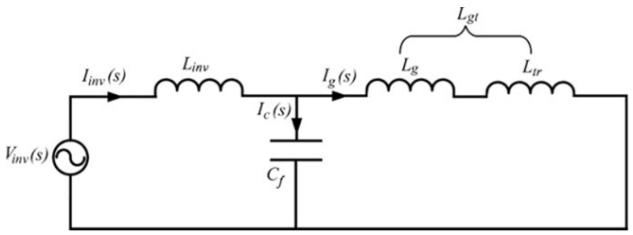

Fig. 2.3 Per phase equivalent circuit for a grid-connected PWM inverter with LCL-filter

Design of Three-Phase LCL-Filter

$$\frac{I_c(s)}{I_g(s)} = L_{gt}C_f s^2 \quad (5)$$

Where vinv, iinv, ig, and ic, respectively, stand for the time-domain representations of the inverter voltage, inverter current, grid current, and filter capacitor current, while their capitalised notations stand for the s-domain representations. Inverter-side filter inductor, grid-side filter inductor, and transformer inductor are all abbreviated as Linv, Lg, and Ltr, respectively.

Modelling the PWM inverter as a linear amplifier with a delay is possible. The delay and the current PI controller can be coupled. The PI current controllers' transfer-function in the dq reference frame is:

$$G_c(s) = K_p V_{dc}\left(1 + \frac{1}{\tau_c s}\right) (6)$$

where Kp, c, and Vdc stand for the proportional gain, integral time constant, and dc-link voltage, respectively, of the PI controller.

D. *Grid-Current Feedback*

The control block diagram for a three-phase PWM inverter using an LCL filter and grid current feedback is shown in Fig 2.3. The system open-loop transfer function is given by Eqs. (4) and (6) as follows:

$$\frac{I_g(s)}{I_g^*(s) - I_g(s)} = G_c(s)G_p(s)$$

$$= \frac{K_p V_{dc}\left(s + \frac{1}{\tau_c}\right)}{L_{inv}L_{gt}C_f s^4 + (L_{inv} + L_{gt})s^2} (7)$$

Equation (7) demonstrates that the typical equation lacks a third order term, which suggests that:

1. It is difficult for the entire closed-loop system to be stable.
2. Even when a passive element (R) is included, it is sometimes insufficient to guarantee a well-damped plant.
3. The plant's dynamic response time and control bandwidth are both small.

To improve this method, external passive or active dampening can be used to stop infinite gain at the LCL response frequency.

E. *Three Phase Grid-connected Inverter Mathematical Model*

Fig2.4 depicts the primary the three phase grid-connected inverter's circuit, where the e e a c denotes the three-phase power network's voltage and the i i a c denotes the positive direction of the parallel grid current, as illustrated in the figure. The phase inductance is L, while the filter inductor's equivalent resistance is R. When the grid voltage is in three-phase symmetry, the three-phase circuit is independent of one another and the output voltage of the inverter bridge is v v a c, omitting the high-frequency component.

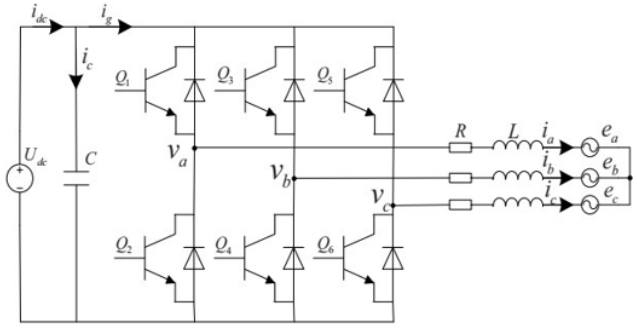

Fig. 2.4. Three phase grid-connected inverter topology

$$\begin{bmatrix} L\frac{di_a}{dt} \\ L\frac{di_b}{dt} \\ L\frac{di_c}{dt} \end{bmatrix} = \begin{bmatrix} -R & 0 & 0 \\ 0 & -R & 0 \\ 0 & 0 & -R \end{bmatrix} \begin{bmatrix} i_a \\ i_b \\ i_c \end{bmatrix} - \begin{bmatrix} 1 & 0 & 0 \\ 0 & 1 & 0 \\ 0 & 0 & 1 \end{bmatrix} \begin{bmatrix} v_a \\ v_b \\ v_c \end{bmatrix} + \begin{bmatrix} 1 & 0 & 0 \\ 0 & 1 & 0 \\ 0 & 0 & 1 \end{bmatrix} \begin{bmatrix} e_a \\ e_b \\ e_c \end{bmatrix} (8)$$

Using coordinate transformation, the physical quantities in static coordinates can be converted into physical quantities in the two-phase synchronous rotating dq coordinate system, as shown in (8).

$$\begin{bmatrix} L\frac{di_d}{dt} \\ L\frac{di_q}{dt} \end{bmatrix} = \begin{bmatrix} -R & wL \\ wL & -R \end{bmatrix} \begin{bmatrix} i_d \\ i_q \end{bmatrix} - \begin{bmatrix} 1 & 0 \\ 0 & 1 \end{bmatrix} \begin{bmatrix} v_d \\ v_q \end{bmatrix} + \begin{bmatrix} 1 & 0 \\ 0 & 1 \end{bmatrix} \begin{bmatrix} e_d \\ e_q \end{bmatrix} (9)$$

F. Mathematical Model of the Proposed GTO

The suggested GTO algorithm imitates the actions taken by huge trevallies when seabirds are on the prowl. As a result, the optimisation processes of the suggested GTO algorithm are divided into three steps: a thorough search utilising Levy flight, a phase to choose the hunting region, and a step where the hunter chases and attacks the prey by leaping out of the water. As a result, the first two phases represent the GTO's exploration phase, whereas the third step represents the GTO's exploitation phase.

Step 1: Extensive Search

If we take into account the characteristics of huge trevallies—which, as was already noted, may traverse great distances for their daily diet. Therefore, utilising (9), huge trevally foraging movement patterns are recreated in this stage.

$$X(t+1) = Best_p \times R + ((Maximum - Minimum) \times R + Minimum) \times Levy(Dim) (10)$$

X(t + 1) is the giant trevally position vector for the following iteration, and BestP is the current search space that the giant trevallies have chosen based on the best location they found during their last search. R is a random number that has a value between 0 and 1. The alleged distribution of Levy controls the step sizes of the Levy flight, a particular form of non-Gaussian stochastic process, which goes by the notation Levy(Dim). The algorithm is helped by the occasional huge steps it needs to complete a global search. staying away from local optima and an increase in convergence rate are two other benefits of adopting Levy flight.

In this context, it is important to note that various studies have demonstrated that a wide range of species, particularly marine predators, exhibit the behaviour of Levy flight. Use (10 to calculate Levy(Dim).

$$Levy(Dim) = step \times \frac{u \times \sigma}{\frac{1}{\beta}} (11)$$

In this example, is the index of the Levy flight distribution function, which can take values ranging from 0 to 2 but has been set to 1.5. u and v are random numbers normally distributed in the range (0; 1), step is the step size, which is fixed at 0.01, and is the Levy flight distribution function. is determined by using (11).

$$\sigma = \left(\frac{T(1+\beta) \times sine\left(\frac{\pi\beta}{2}\right)}{T\left(\frac{1+\beta}{2}\right) \times \beta \times 2^{\left(\frac{\beta-1}{2}\right)}} \right) (12)$$

Step 2: Choosing Area

During the stage of choosing an area, gigantic trevallies locate and pick the location

where they can find the most food (seabirds) inside the chosen search zone. Mathematically simulating this behaviour is Equation (12).

$$(t+1) = Best_P \times A \times R + Mean_{Info} - Xi(t) \times R \quad (13)$$

A is a position-change control parameter with a range of 0.3 to 0.4, and X(t C 1) is the position vector of enormous trevallies in the subsequent iteration t. The location of the enormous trevally i at time t (the current iteration) is Xi.t/. As for the enormous trevallies, which refers to the mean, implies that all of the data from the prior points has been used to calculate (13).

$$Mean_{Info} = \frac{1}{N}\sum_{i=1}^{N} Xi(t) \quad (14)$$

Step 3: Attacking

After identifying the ideal hunting place in the prior phase. The trevally begins pursuing the bird (prey) in this phase, which corresponds to the GTO's exploitation (intensification) stage. The trevally attacks the bird by doing an acrobatic jump out of the water and snatching it when it is close enough.

III. RESULT AND DISCUSSION

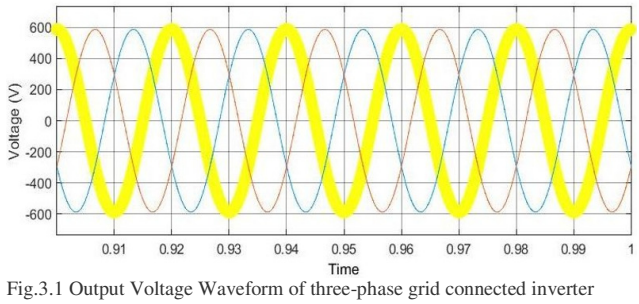

Fig.3.1 Output Voltage Waveform of three-phase grid connected inverter

In fig 3.1 shows the output voltage waveform of three-phase grid connected inverter. This waveform is plotted between time and voltage(V). The actual current is same as the reference current. It shows the voltage waveform from the three phase grid connected inverter.

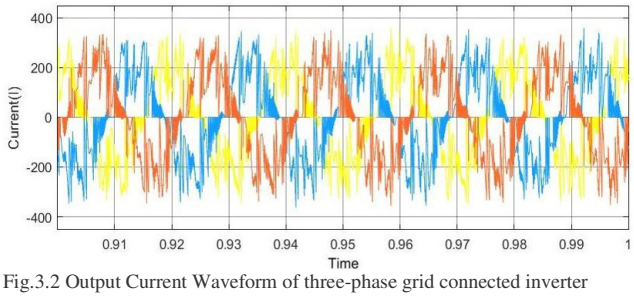

Fig.3.2 Output Current Waveform of three-phase grid connected inverter

In fig 3.2 shows the output current waveform of three-phase grid connected inverter, the actual current is same as the reference current. This waveform is plotted between time and current(I). The actual current is same as the reference current. It shows the current waveform from the threephase grid connected inverter.

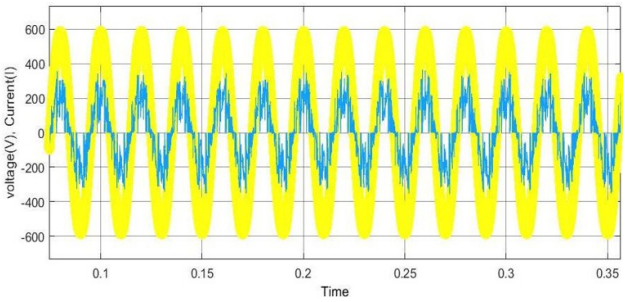

Fig.3.3 Output of Voltage and Current in one particular phase

In fig 3.3 shows the output of voltage and current is in one particular phase, since we are sending only active current. This waveform is plotted between time and voltage(V) current(I). The voltage and current in one particular phase, we are sending active current.

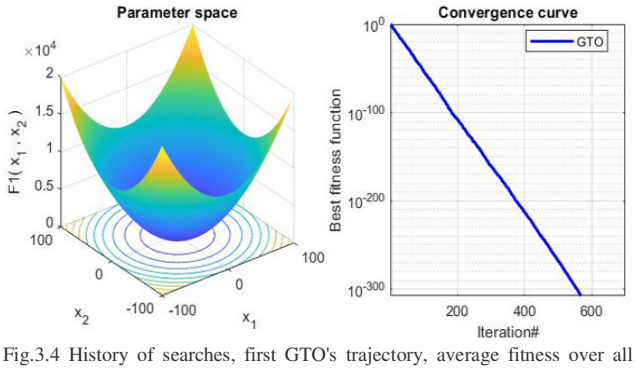

Fig.3.4 History of searches, first GTO's trajectory, average fitness over all GTO, and convergence analysis.

We note the fitness of the leading giant trevally in this iteration and present their convergence

curves in Fig 3.4. A steady decline in fitness suggests that the GTO algorithm has reached convergence. The faster degradation can be seen in convergence curves as well, for the previously described reason, which is equally significant to note.

IV. CONCLUSIONS

This study models the three-phase LCL filter and the grid using complex vectors when A synchronous frame PI controller manages the grid current. A complex grid current vector in a synchronous dq reference frame is used to generate the controller. The complex vector of grid current's closed-loop function with respect to the complex vector of command current includes a synchronous frame PI controller. Benefits of the complex vector GCI model include the ability to show the GCI system's d- and q-axis components in a single block diagram and a lowered order of the GCI system from 6th to 3rd order. With the use of complex vector root loci and complicated vector frequency response function and PI controller effectiveness and the impact of the tuning parameter are studied. System performance can be evaluated using just one plot of the root locus and frequency response function thanks to the complexity vector model. Given a specification for a 10 kW three-phase grid-connected inverter, Kp = 5 is the ideal tuning value for Ki/Kp = 20 and 200. This thesis introduces a unique swarm-based metaheuristic algorithm that draws inspiration from the giant trevally's hunting strategy. Three steps made up the suggested algorithm, known as the gigantic Trevally Optimizer (GTO), which simulated gigantic trevallies' behaviour. Additionally shown are the system's step reaction and the MATLAB-simulated findings. THD has been decreased by a level of 2.40%, which is less than 5%. Instead of using trial and error, it is advantageous to adjust the synchronous PI controller's gain parameters using a sophisticated vector model based on a real-world system.

ACKNOWLEDGMENT

This work was supported by Department of Electrical and Electronics Engineering, Arunachala College of Engineering for Women Manavilai, Vellichanthai.

REFERENCES

[1] J. Xu, H. Qian, S. Bian, Y. Hu and S. Xie, "Comparative study of single-phase phase-locked loops for grid-connected inverters under non-ideal grid conditions," in CSEE Journal of Power and Energy Systems, vol. 8, no. 1, pp. 155-164, Jan. 2022, doi: 10.17775/CSEEJPES.2019.02390.

[2] Q. Yan, X. Wu, X. Yuan and Y. Geng, "An Improved Grid-Voltage Feedforward Strategy for High-Power Three-Phase Grid-Connected Inverters Based on the Simplified Repetitive Predictor," in IEEE Transactions on Power Electronics, vol. 31, no. 5, pp. 3880-3897, May 2016, doi: 10.1109/TPEL.2015.2461632.

[3] X. Guo, X. Zhang, B. Wang, W. Wu and J. M. Guerrero, "Asymmetrical Grid Fault Ride-Through Strategy of Three-Phase Grid-Connected Inverter Considering Network Impedance Impact in Low-Voltage Grid," in IEEE Transactions on Power Electronics, vol. 29, no. 3, pp. 1064-1068, March 2014, doi: 10.1109/TPEL.2013.2278030.

[4] T. Uzzaman, U. Kim and W. Choi, "A Novel Frequency Locked Loop With Current Harmonic Elimination Method for the Three-Phase Grid-Connected Inverter," in IEEE Access, vol. 10, pp. 32870-32878, 2022, doi: 10.1109/ACCESS.2022.3160743.

[5] K. -J. Lee, B. -G. Park, R. -Y. Kim and D. -S. Hyun, "Robust Predictive Current Controller Based on a Disturbance Estimator in a Three-Phase Grid-Connected Inverter," in IEEE Transactions on Power Electronics, vol. 27, no. 1, pp. 276-283, Jan. 2012, doi: 10.1109/TPEL.2011.2157706.

[6] A. Hintz, U. R. Prasanna and K. Rajashekara, "Comparative Study of the Three- Phase Grid-Connected Inverter Sharing Unbalanced Three-Phase and/or Single- Phase systems," in IEEE Transactions on Industry Applications, vol. 52, no. 6, pp. 5156-5164, Nov.-Dec. 2016, doi: 10.1109/TIA.2016.2593680.

[7] B. Zhang, X. Du, J. Zhao, J. Zhou and X. Zou, "Impedance modeling and stability analysis of a three-phase three-level NPC inverter connected to the grid," in CSEE Journal of Power and Energy Systems, vol. 6, no. 2, pp. 270-278, June 2020, doi: 10.17775/CSEEJPES.2019.02620.

[8] M. Alqatamin, J. Latham, Z. T. Smith, B. M. Grainger and M. L. McIntyre, "Current Control of a Three-Phase, Grid-Connected Inverter in the Presence of Unknown Grid Parameters Without a Phase-Locked Loop," in IEEE Journal of Emerging and Selected Topics in Power Electronics, vol. 9, no. 3, pp. 3127-3136, June 2021, doi: 10.1109/JESTPE.2020.3001153.

[9] R. Zhao, C. Wang, P. C. Loh, Q. Yan, H. Xu and F. Blaabjerg, "A Practical Core Loss Estimation Method for Three-Phase Three-Level Grid-Connected Inverters," in IEEE Transactions on Power Electronics, vol. 35, no. 3, pp. 2263-2267, March 2020, doi: 10.1109/TPEL.2019.2943875.

[10] O. Kukrer, S. Bayhan and H. Komurcugil, "Model-Based Current Control Strategy With Virtual Time Constant for Improved Dynamic Response of Three-Phase Grid- Connected VSI," in IEEE Transactions on Industrial Electronics, vol. 66, no. 6, pp. 4156-4165, June 2019, doi: 10.1109/TIE.2018.2863195.

[11] Y. Yu and X. Hu, "Active Disturbance Rejection Control Strategy for Grid- Connected Photovoltaic Inverter Based on Virtual Synchronous Generator," in IEEE Access, vol. 7, pp. 17328-17336, 2019, doi: 10.1109/ACCESS.2019.2894786.

[12] R. Bisht, R. Bhattarai, S. Subramaniam and S. Kamalasadan, "A Novel Synchronously Rotating Reference Frame Based Adaptive Control Architecture for Enhanced Grid Support Functions of Single-Phase

Inverters," in IEEE Transactions on Industry Applications, vol. 56, no. 4, pp. 4288-4298, July-Aug. 2020, doi: 10.1109/TIA.2020.2994879.

[13] X. Quan, "Improved Dynamic Response Design for Proportional Resonant Control Applied to Three-Phase Grid-Forming Inverter," in IEEE Transactions on Industrial Electronics, vol. 68, no. 10, pp. 9919-9930, Oct. 2021, doi: 10.1109/TIE.2020.3021654.

[14] M. Berg, H. Alenius and T. Roinila, "Rapid Multivariable Identification of Grid Impedance in DQ Domain Considering Impedance Coupling," in IEEE Journal of Emerging and Selected Topics in Power Electronics, vol. 10, no. 3, pp. 2710-2721, June 2022, doi: 10.1109/JESTPE.2020.3041446.

[15] A. B. Shitole et al., "Grid Interfaced Distributed Generation System With Modified Current Control Loop Using Adaptive Synchronization Technique," in IEEE Transactions on Industrial Informatics, vol. 13, no. 5, pp. 2634-2644, Oct. 2017, doi: 10.1109/TII.2017.2665477.

